

Bidirectional Ray Tracing for the Integration of Illumination by the Quasi-Monte Carlo Method

A. G. Voloboi, V. A. Galaktionov, K. A. Dmitriev, and E. A. Kopylov

*Keldysh Institute of Applied Mathematics, Russian Academy of Sciences,
Miusskaya pl. 4, Moscow, 125047 Russia
e-mail: oek@gin.keldysh.ru*

Received April 23, 2004

Abstract—Algorithms used to generate physically accurate images are usually based on the Monte Carlo methods for the forward and backward ray tracing. These methods are used to numerically solve the light energy transport equation (the rendering equation). Stochastic methods are used because the integration is performed in a high-dimensional space, and the convergence rate of the Monte Carlo methods is independent of the dimension. Nevertheless, modern studies are focused on quasi-random samples that depend on the dimension of the integration space and make it possible to achieve, under certain conditions, a high rate of convergence, which is necessary for interactive applications. In this paper, an approach to the development of an algorithm for the bidirectional ray tracing is suggested that reduces the overheads of the quasi-Monte Carlo integration caused by the high effective dimension and discontinuity of the integrand in the rendering equation. The pseudorandom and quasi-random integration methods are compared using the rendering equations that have analytical solutions.

1. INTRODUCTION

Physically accurate modeling of illumination finds applications in architecture, design, cinematography, design of lighting devices, and in the construction of photorealistic images in virtual reality. Despite the advances in computer hardware, the time required to produce realistic images remains too large for interactive applications. The graphics hardware, which ensures the fast rendering of 2D and 3D graphics, is not designed for physically accurate modeling of illumination; therefore, algorithmic methods of image generation remain one of the problems in modern computer graphics.

Algorithms of realistic image generation, which use accurate illumination models, are based on solving the rendering equation [1]. This equation describes the radiance, $L(\vec{x}, \omega)$, of the point \vec{x} of the surface in the direction ω ; it has the recurrent form

$$K(\vec{x}, \omega) = L^e(\vec{x}, \omega) + IL(\vec{x}, \omega), \quad (1)$$

where L^e is the emittance of the point of the surface due to the direct illumination, and the integral operator I , which takes into account the visibility of the scene points $h(\vec{x}, \omega)$, describes the interaction of the light arriving from other illuminated surfaces (Fig. 1):

$$IL(\vec{x}, \omega) = \int_{\Omega} L(h(\vec{x}, -\omega'), \omega') f_r(\omega', \vec{x}, \omega) \cos \theta' d\omega'. \quad (2)$$

In this equation, the optical properties of the surface are given by the bidirectional reflectance (refraction) distribution function f_r (BRDF), which is the ratio of the incoming and outgoing radiant power:

$$f_r(\omega', \vec{x}, \omega) = \frac{\partial L(\vec{x}, \omega)}{\partial L(\vec{x}, \omega')}. \quad (3)$$

Along with the energy forms of the rendering equation (1), (2), one can consider its dual form describing the potential visibility function $W(\vec{y}, \omega')$ (this function expresses the visibility from the observation point \vec{y} in the direction ω' (Fig. 2)):

$$W(\vec{y}, \omega') = W^e(\vec{y}, \omega') + I^*W(\vec{y}, \omega'). \quad (4)$$

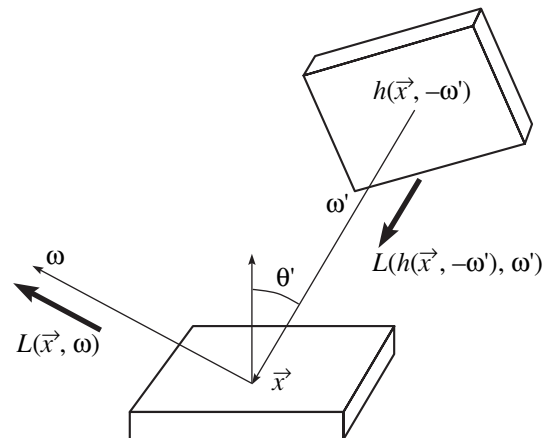


Fig. 1. Components of the rendering equation.

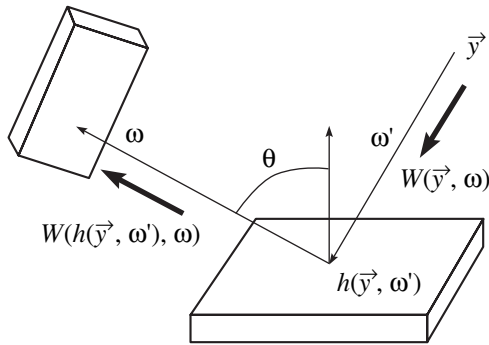


Fig. 2. Components of the potential equation.

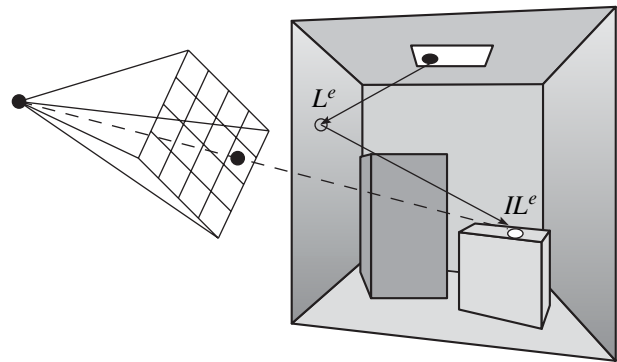


Fig. 3. Forward ray tracing.

Here, W^e is the direct visibility in the direction of observation, and the integral operator I^* as adjoint of I :

$$I^* W(\vec{y}, \omega') = \int_{\Omega} W(h(\vec{y}, \omega'), \omega) f_r^*(\omega, h(\vec{y}, \omega'), \omega') \cos \theta d\omega \quad (5)$$

The methods of image generation based on solving the rendering equation (1) for the radiance are called the forward methods, while those based on the potential equation (4) are called the backward methods. A general classification of methods for solving integral equations is given in [2]. These methods are classified into three types: *inversion*, *iteration*, and *expansion*. The expansion method is the most flexible and universal one: it is analyzed in [3]. As applied to the rendering equation (1) and the potential equation (4), the expansion method reduces the solution to finding certain integral sums (see Table 1).

The *forward ray tracing* uses the expansion method to solve Eq. (2); it is called the photon tracing method. The representation of the propagation of photons in the form of the infinite series $\sum_{i=0}^{\infty} I^i L^e$ has a simple intuitive meaning (see Fig. 3).

L^e is the contribution of the direct light, $I^1 L^e$ is the contribution of light that comes from a light source once reflected, $I^2 L^e$ is the contribution of the twice reflected light, etc. It is easily seen that the dimension of the term $I^d L^e$ is $2d + 2$, which results in a high-dimensional integral. The result of the forward photon tracing is a photon or illumination map given on a grid. It is rendered using a standard graphical interface (for example, OpenGL).

The *ray backtracing* also called path tracing gives a solution to the potential equation (5). Every path being traced begins at the observation point and makes contribution to the corresponding pixel of the image (Fig. 4); thus, the image is formed on the screen. Being dual to the photon tracing method, the path tracing has the same dimension.

The expansion method is often implemented with the use of the Monte Carlo method, which is characterized by the independence of integral dimension. The error of this method is a random noise, which is independent of the number of reflections and refractions. For N traced rays, the error is $O(N^{-1/2})$. Figure 5 shows the images obtained by the Monte Carlo method for the first n terms of the series (for $n = 0$, $n = 1$, $n = 2$, and $n = 4$).

It is known that the sample in the classical Monte Carlo method need not necessarily be random in order for the integral sum to converge to the integral being evaluated. Many nonrandom (so-called quasi-random) number sequences, for example, LP_{τ} -sequences [4], are known that under certain conditions ensure a higher rate of convergence of the integral sums. The studies [5, 6] are devoted to the use of quasi-Monte Carlo integration in the implementation of the expansion method.

Bidirectional methods are widely used in expansion algorithms for the generation of realistic images. These methods combine the forward and backward ray tracing. An efficient implementation of bidirectional methods is achieved by tracing only the rays that make a substantial contribution to the image being generated. The implementation of the bidirectional ray tracing assumes that an optimization problem is solved to minimize the number of traced rays that ultimately transfer energy

Table 1. The expansion method

For the rendering equation (forward tracing)	For the potential equation (backward tracing)
$L = L^e + IL \Rightarrow$	$W = W^e + I^* W \Rightarrow$
$L = L^e + I(L^e + IL) \Rightarrow$	$W = W^e + I^*(W^e + I^* W) \Rightarrow$
$L = L^e + IL^e + I^2 L \Rightarrow$	$W = W^e + I^* W^e + I^{*2} W \Rightarrow$
$L = \sum_{i=0}^n I^i L^e + I^{n+1} L \Rightarrow$	$W = \sum_{i=0}^n I^{*i} W^e + I^{*n+1} W \Rightarrow$
$L \xrightarrow[\lim_{n \rightarrow \infty} I^{n+1} L = 0]{} \sum_{i=0}^{\infty} I^i L^e$	$W \xrightarrow[\lim_{n \rightarrow \infty} I^{*n+1} W = 0]{} \sum_{i=0}^{\infty} I^{*i} W^e$

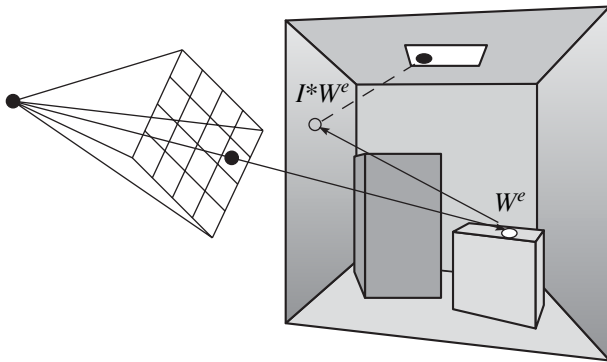


Fig. 4. Ray backtracing.

from the light source to the observer. Various approaches to the construction of an algorithm for the bidirectional ray tracing are discussed in [7–9].

The change to the quasi-Monte Carlo integration is formally very simple: the pseudorandom number generator used in the classical Monte Carlo method is replaced by a quasi-random number generator. Although the advantages of the use of a quasi-random sequence for the integration are obvious, the successful application depends on the dimension of the integration domain and the smoothness of the integrand. In this paper, we develop an algorithm for the bidirectional ray tracing that minimizes the overhead of quasi-Monte Carlo integration caused by the high dimension of the integration domain and discontinuity of the integrand.

2. THE COMPONENT SEPARATION METHOD

The major contribution to the violation of smoothness is made by the direct illumination component, especially if it comes from point or remote light sources, because they cast sharp shadows and create large gradients. The computation of direct illumination

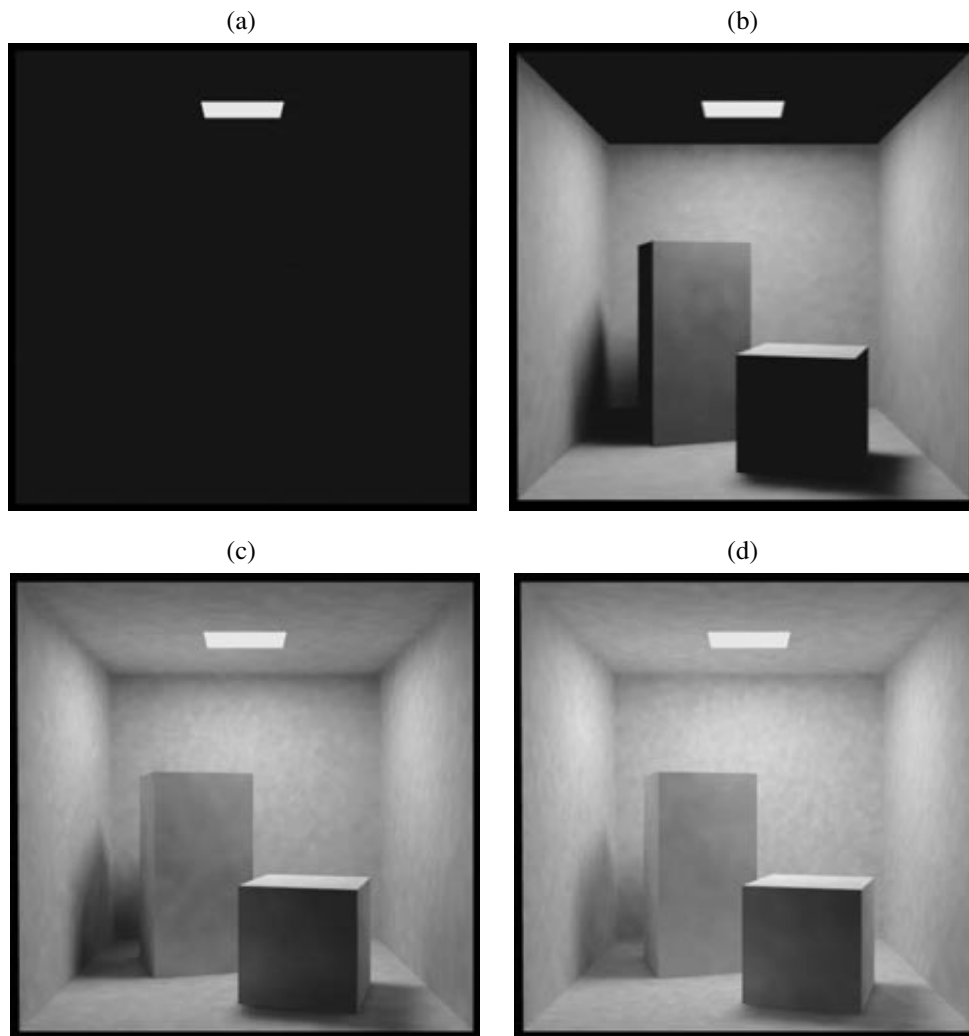


Fig. 5. Forward ray tracing. (a) $L = L^e$; (b) $L = L^e + IL^e$; (c) $L = L^e + IL^e + I^2L^e$; (d) $L = \sum_{i=0}^4 I^i L^e$.

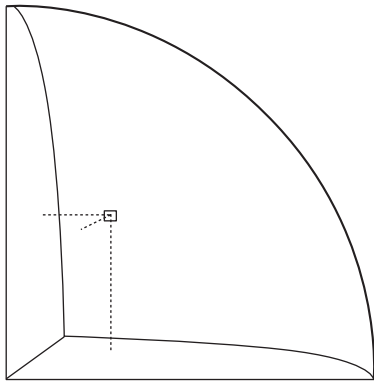


Fig. 6. Octant of a sphere.

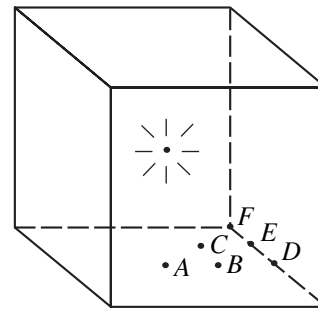


Fig. 7. Diffusive cube.

is fairly simple, it is reasonable to eliminate point light sources from the expansion method altogether.

Consider the integral sum for the rendering equation in the expansion method (Table 1):

$$L \approx \sum_{i=0}^{\infty} I^i L^e = L^e + \sum_{i=1}^{\infty} I^i L^e = L^{ep} + L^{er} + \sum_{i=1}^{\infty} I^i L^e.$$

Here L^{ep} is the luminous intensity of the light sources for which the direct illumination component can be computed analytically on the surfaces of the scene, and L^{er} is the luminous intensity of all other sources, for which the direct illumination is computed by photon tracing. Replacing the luminous intensity of the point light sources by the luminous intensity of the grid elements corresponding to the illuminated surfaces, we obtain a new set of light sources

$$L^{e*} = L^e - L^{ep} + IL^{ep}.$$

Thus, the numerical integration is applied to the modified rendering equation

$$L \approx L^{ep} + \sum_{i=0}^{\infty} I^i L^{e*}$$

with a smoother integrand.

It was noted in [10] that, for diffusive surfaces, for which the luminous intensity is independent of the direction of the incident light, it is obviously sufficient to store only the quantitative component of the luminous intensity IL^{ep} for each element of the grid. For nondiffusive surfaces, IL^{ep} depends on the direction of the incident light L^{ep} . In this case, it is reasonable to separately store the direct illumination received by each element of the grid from each pointwise light source. Then, the desired IL^{ep} can be computed by demand for the desired light source and the corresponding direction L^{ep} on the basis of the stored data. In [11], one can find an example of the implementation of the stochastic photon tracing algorithm in which the direct illumination represented by a piecewise linear function on a tri-

angular grid is recalculated into the probability distribution function p_i to pseudorandomly generate the secondary photons. For a prescribed constraint imposed on the maximal size of triangular cell and an adaptive algorithm for the generation of a triangular grid for direct illumination, we construct a discrete cumulative distribution function p_i in the form of an array of dimension $N = \prod_{i=1}^L N(i)$, where L is the number of light sources for which the direct illumination is calculated analytically and $N(i)$ is the number of triangular cells for which the illumination from the i th light source is calculated.

Note that when the probability distribution function is constructed to select a triangle–source pair, the possible absorption of light is taken into account. Thus, the probability of absorption at the stage of an event generation is minimized; therefore, the method does not waste time and quasi-random numbers to trace the photons that will be surely absorbed before they contribute to the illumination map. An excessive use of members of the quasi-random sequence results in the degradation of performance due to two reasons: the effective dimension of the algorithm increases, and the problem becomes more “discontinuous” [12].

3. DECREASING THE EFFECTIVE DIMENSION OF THE PHOTON TRACING PROBLEM

The dimension of the expansion method for solving the rendering equation is infinite independently of whether it is used in the context of the bidirectional ray tracing algorithm or separately. Theoretically, the trajectory of a photon or a backward path can consist of an infinite number of segments, and it is impossible to a priori determine the dimension of the random vector $\{\eta_1, \dots, \eta_i\}$ that is required to realize such a trajectory. For example, η_0 corresponds to the choice of the source–triangle pair, η_1 and η_2 correspond to the choice of a point in the triangle, η_3 corresponds to the choice of an alternative event (reflection, or refraction, or absorption, depending on the optical properties of the surface), η_4 and η_5 correspond to the choice of the photon emission

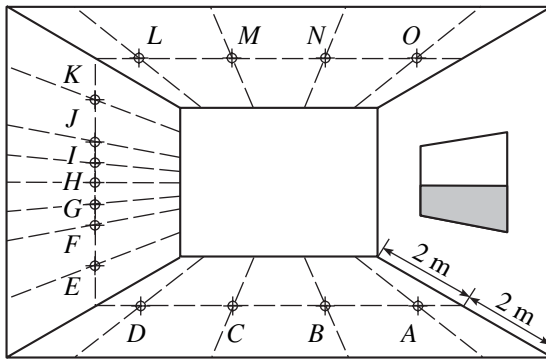


Fig. 8. CIE TC.3.33 test.

direction, and so on. Actually, photons are absorbed, and the probability of an infinitely long trajectory is zero. Therefore, we use the concept of effective dimension defined as the average (rather than maximal) number of elements η_i required to trace a single photon (a path).

In the process of tracing, some events assume a choice of an outcome among a number of possible outcomes; thus, the probability of such an event has a discrete density distribution. It is well known that when discrete events are chosen, one may use the same pseudorandom value several times applying a renormalization procedure. This method, which was first proposed to accelerate the random number generator [12], is called the *modified superposition method*. Formally, if a discrete event depends on whether or not a quasi-random number s falls into the interval $[a, b)$, the renormalization means that the next random number s' can be obtained by

$$s' = (s - a)/(b - a)$$

without increasing the effective dimension of the algorithm.

It must be taken into account that the successive use of the modified superposition method several times and its use for a large number of possible events results in a

nonuniform distribution of the quasi-random numbers. In this case, the advantages of the quasi-Monte Carlo integration in terms of the rate of convergence are lost. Then, one has to abandon the modified superposition method.

To reduce the effective dimension of the ray tracing algorithm, we must do away with rejection sampling methods. Conventionally, such methods are used generate directions on the basis of photometric characteristics of the light sources and diffusive properties of surfaces specified by the bidirectional reflectance function. An example of replacing the rejection sampling method by the inverse function method is presented in [13].

The effective dimension of the quasi-Monte Carlo tracing algorithm can be reduced by using random events instead of quasi-random ones if this does not significantly affect the quasi-random nature of the photon trajectory selection, which accelerates the convergence of the integral sum.

We used this kind of randomization to select a photon emission point within a triangle. If the area of the triangles is small, the influence of the randomization on the selection of trajectories is insignificant, and the advantages of the quasi-Monte Carlo method in terms of the convergence rate are retained. The effective dimension of the quasi-Monte Carlo integration is then reduced by two units. In addition, the randomization in the selection of the emission point within a triangle allows one to use the statistical techniques to evaluate the accuracy of modeling.

4. THE BIDIRECTIONAL RAY TRACING METHOD

The techniques outlined above make it possible to reduce the effective dimension of the photon tracing algorithm and thus improve the efficiency of the use of the quasi-Monte Carlo integration for solving the rendering equation by the expansion method. We may

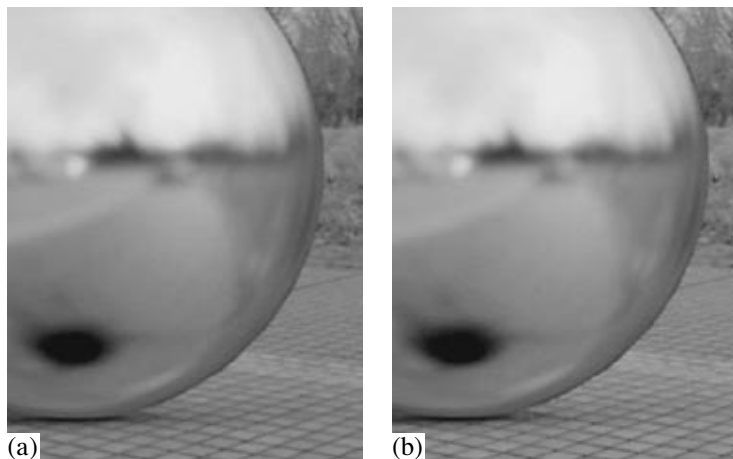


Fig. 9. (a) Pseudo-Monte Carlo integration; (b) Quasi-Monte Carlo integration.

assume that the photon tracing based on the use of quasi-random number sequences can efficiently produce an illumination map that is independent of the position of the camera and in which the contribution of photons with a low effective dimension is evaluated most accurately. We use the triangular grid that coincides with the initial triangulation of the scene surfaces.

The ray backtracing in the proposed bidirectional tracing does not require integration. The paths from the camera are traced through the screen pixel until they intersect a scene surface, where the contribution of the direct illumination and of the secondary illumination from the illumination map are evaluated, and the next iteration I_{spec}^* is constructed for the tree of uniquely determined specularly reflected or refracted paths:

$$W \approx \sum_{i=0}^{\infty} I^{*i} W^e \approx W^e + \sum_{i=0}^N \langle L^{ep}, I_{\text{spec}}^{*i} W^e \rangle + \sum_{i=0}^N \langle L - L^{ep}, I_{\text{spec}}^{*i} W^e \rangle.$$

Here, N is maximum allowed depth of the tracing tree, and the operator $\langle u, v \rangle$ represents the transfer of the light energy that is registered in the illumination map for the trajectories of photons u in the backward direction v from the camera. The computation of the illumination map is independent of the position of the camera, and the construction of the next iteration I_{spec}^* terminates on diffusive surfaces. The advantage of backtracing with the use of the specular ray tree is that the image can be obtained very quickly when the position of the camera changes. Disadvantages of this approach that affect the accuracy of the resulting images are as follows.

1. An element of the illumination map approximates the illumination accumulated on a triangular grid. This representation is rather coarse, and it gives acceptable results only for smooth secondary illumination functions.

2. As a rule, the illumination map does not contain information about the distribution of directions of the incident photons; therefore, the transformation $\langle L - L^{ep}, W^e \rangle$ of the accumulated illumination into the luminous intensity yields an exact value only for surfaces with perfectly diffusive properties. For the optical properties represented by bidirectional reflectance (refraction) functions, the account for the illumination map results in errors.

3. The direct use of the inaccurate value of the illumination $L - L^{ep}$ accumulated on an element of the map is impractical. The accuracy of quasi-Monte Carlo integration used in the photon tracing can be different for different areas of the map due to the high effective dimension, insufficient illumination, or specific features of photon propagation.

Table 2. Results of the photon tracing

Time (s)	Pseudoerror (%)	Quasi-error (%)	Acceleration (quasi/pseudo)
6	4.604	6.45	0.71
12	4.356	4.488	0.97
24	4.591	4.728	0.97
48	4.09	2.181	1.88
96	5.141	2.228	2.31
192	1.564	0.914	1.71
384	1.627	0.39	4.17

Table 3. Results of the bidirectional tracing

Time (s)	Pseudoerror (%)	Quasi-error (%)	Acceleration (quasi/pseudo)
6	43.16	7.05	8.17
12	11.64	2.75	5.65
24	8.78	2.45	4.79
48	5.69	2.08	3.65
96	5.05	1.87	3.60
192	3.26	1.39	3.12
384	2.69	1.37	2.62

The increase of the backtracing dimension can eliminate these disadvantages, but it slows the computations because it uses the full integration. We believe that it is best to use quasi-Monte Carlo integration while slightly increasing the backtracing dimension:

$$W \approx \sum_{i=0}^{\infty} I^{*i} W^e \approx W^e + \langle L^{ep}, I^* W^e \rangle + \langle L - L^{ep}, I^* W^e \rangle + \sum_{i=1}^N \langle L^{ep}, I_{\text{spec}}^{*i} W^e \rangle + \sum_{i=1}^N \langle L - L^{ep}, I_{\text{spec}}^{*i} W^e \rangle.$$

On the one hand, the use of the integral operator I^* in the ray backtracing allows one to considerably improve the accuracy of modeling. On the other hand, the low-dimensional quasi-Monte Carlo integration of the smooth secondary illumination accumulated on the map ensures a high rate of convergence.

5. RESULTS AND DISCUSSION

We implemented the bidirectional ray tracing algorithm that makes an efficient use of quasi-Monte Carlo integration for high dimensions and for nonsmooth integrands.

The comparison of the quasi-Monte Carlo integration based on LP $_{\tau}$ -sequences [4] with the conventional Monte Carlo method both for photon tracing and bidirectional ray tracing was performed for scenes in which the total luminance can be calculated analytically at certain test points.

5.1. Octant of a Sphere

The secondary illumination can be calculated exactly if the form factor of all pairs of points is the same [14]. The scene consists of the 1/8th part of the unit diffusive sphere cut by three specular coordinate planes with the reflectance 1.0, 0.8, 0.6 and of a homogeneous point light source with the luminous intensity of 100 cd inside the spherical segment at the point with the coordinates (0.2, 0.4, 0.6). The generalized form factor, which characterizes the transfer of energy between diffusive and diffusive-specular-diffusive surfaces is the same for all pairs of points of the part of the sphere under consideration. The theoretical value of the total illumination at the center of the octant at the point $\left(\frac{1}{\sqrt{3}}, \frac{1}{\sqrt{3}}, \frac{1}{\sqrt{3}}\right)$ is 1353.247 lx. Table 2 shows the errors of modeling the illumination by the photon tracing method. The effective dimension of the photon tracing for the octant of a sphere is 4.3.

5.2. Diffusive Cube

The scene is cube of the size 10m \times 10 m \times 10 m with a point light source with the luminous intensity of 50000 cd at its center. This light produces the direct illumination of 2000 lx at the nearest points of the cube faces (the points A). The light propagates diffusively inside the cube without leaving it. The reflectance of the diffusive faces is 2/3. Thus, a large part of illumination is created by the reflected light. Both the light and the cube surface are white.

The theoretical values of the luminous intensity at the six points on the faces (the points A–F) can be found in [14]. Using the symmetry of the scene, we find the difference between the modeled and theoretical values on the 5-by-5 grid on each internal surface of the cube faces. Thus, the error is calculated in the L_2 norm on the basis of 150 points.

Table 3 shows the errors of modeling the illumination by the bidirectional ray tracing method.

The effective dimension of the photon tracing method for the diffusive cube is six and that of the backward ray tracing, two.

5.3. CIE TC.3.33 Test

This test was proposed in [15] to analyze application programs aimed at the design of daylight illumination in rooms. The scene is an absolutely black room with an open window and a plane that imitates a ground with a

30% reflectance. The theoretical values are calculated at the points A–Q provided that the homogeneous luminous intensity of celestial hemisphere is 1000 cd/m².

We compared the results produced by the bidirectional ray tracing methods that differ in the implementation of the path backtracing. The average error of the algorithm that does not perform integration at the backtracing stage was 15%, and the biggest error of 48.4% was at the point J. The average error of the backtracing algorithm based on the quasi-Monte Carlo integration of the minimal dimension was 2%, and the maximum error of 7.2% was at the point C. Moreover, the latter algorithm proved to be about 100 times faster than the former one.

5.4. A Sphere with a Bidirectional Reflectance Function

The ray backtracing methods with the quasi-Monte Carlo and pseudo-Monte Carlo integration were compared by solving the problem of color filling a sphere with the silver reflectance properties given the tabulated bidirectional reflectance distribution function (BRDF). The sphere is surrounded by a spherical high dynamic range image (HDRI) used as the source of illumination [16].¹

The initial number of generated rays was 128 per pixel, and the pixel was filled when the error of integration was not greater than 2%. The error of the quasi-Monte Carlo integration was evaluated approximately by dividing the rays being traced into two groups judging by the first quasi-random number. The time taken by the method based on the pseudo-Monte Carlo and quasi-Monte Carlo integration was 179 and 122 seconds, respectively.

6. CONCLUSIONS

An efficient bidirectional ray tracing method based on the quasi-Monte Carlo integration was developed and implemented in the framework of developing a realistic visualization system based on physically accurate optical modeling. On the whole, the results show that the quasi-Monte Carlo method outperforms the conventional pseudo-Monte Carlo method in terms of the convergence rate for the forward and backward ray tracing (tests 5.1 and 5.4). The standard CIE TC.3.33 test 5.3 (the design of daylight illumination in rooms) shows that the use of the minimum dimension ray backtracing is reasonable, and testing the convergence rate of the bidirectional ray tracing (test 5.2) demonstrates the efficiency of the implementation.

The bidirectional ray tracing method was used in several software systems produced by the Intega Inc. company [17].

¹ Full-color images are available in the internet version of this paper at <http://www.keldysh.ru/pages/cgraph/article/dep20/kop2004.pdf>.

ACKNOWLEDGMENTS

This work was supported by the Russian Foundation for Basic Research, project no. 04-01-00520 and by Integra Inc. (Japan).

REFERENCES

1. Kajiya, J.T., The Rendering Equation, *Proc. of the Int. Conf. on Computer Graphics and Interactive Techniques (SIGGRAPH'86)*, 1986, pp. 143–150.
2. Szirmay-Karlos, L., *Monte Carlo Methods in Global Illumination*, Vienna: Institute of Computer Graphics, Vienna University of Technology, 1999.
3. Khodulev, A., Comparison of Two Methods of Global Illumination Analysis, Technical Report of Keldysh Inst. Appl. Math., 1996; <http://www.keldysh.ru/pages/cgraph/articles/index.htm>
4. Sobol', I.M., *Mnogomernye kvadraturnye formuly i funktsii Khaara* (Multidimensional Quadrature Rules and Haar Functions), Moscow: Nauka, 1969.
5. Keller, A., A Quasi-Monte Carlo Algorithm for the Global Illumination in the Radiosity Setting, in *Monte Carlo and Quasi-Monte Carlo Methods in Scientific Computing*, Niederreiter, H. and Shiue, P., Eds., Springer, 1995, pp. 239–251.
6. Szirmay-Karlos, L., Foris, T., Neumann, L., and Csefalvi, B., An Analysis to Quasi-Monte Carlo Integration Applied to the Transillumination Radiosity Method, *Computer Graphics Forum*, 1997, vol. 16, no. 3, pp. 271–281.
7. Lafortune, E.P. and Willems, Y.D., Bi-directional Path Tracing, *Computer Graphics Proc.*, Alvor (Portugal), 1993, pp. 145–153.
8. Veach, E. and Guibas, L.J., Optimally Combining Sampling Techniques for Monte Carlo Rendering, *SIGGRAPH'95 Proc.*, Addison–Wesley, 1995, pp. 77–102.
9. Pattanaik, S.N. and Mudur, S.P., Adjoint Equations and Random Walks for Illumination Computation, *ACM Trans. Graph.*, 1995, vol. 14, pp. 77–102.
10. Castro, F., Martinez, R., and Sbert, M., Quasi-Monte Carlo and Extended First-Shot Improvements to the Multi-Path Method, *Spring Conf. on Computer Graphics*, 1998, pp. 91–102.
11. Kopylov, E.A., An Efficient Method for the Illumination Evaluation Based on the Use of the Probability Distribution Function for Ray Generation, *Graphicon'2002*, pp. 225–229.
12. Sobol', I.M., *Chislennyye metody Monte-Karlo* (Numerical Monte Carlo Methods), Moscow: Nauka, 1973.
13. Dmitriev, K., From Monte Carlo to Quasi-Monte Carlo Methods, *Graphicon'2002*, pp. 53–58.
14. Kopylov, E.A., Khodulev, A.B., and Volevich, V.L., The Comparison of Illumination Maps Technique in Computer Graphics Software, *Graphicon'98*, pp. 146–152.
15. Maamari, F., TC.3.33 List of Proposed Test Cases, *Ecole National des Travaux Publics de l'Etat, Laboratory of Building Sciences, Department of Civil Engineering and Building*, URA CNRS 1652, 2002.
16. Debevec, P., Fong, N., and Lemmon, D., Image-Based Lighting, *SIGGRAPH Course*, 2002, no. 5.
17. <http://www.integra.jp>